

Terahertz radiation in alkali vapor plasmas

Xuan Sun and X.-C. Zhang

Citation: [Applied Physics Letters](#) **104**, 191106 (2014); doi: 10.1063/1.4876602

View online: <http://dx.doi.org/10.1063/1.4876602>

View Table of Contents: <http://scitation.aip.org/content/aip/journal/apl/104/19?ver=pdfcov>

Published by the [AIP Publishing](#)

Articles you may be interested in

[Numerical and simulation study of terahertz radiation generation by laser pulses propagating in the extraordinary mode in magnetized plasma](#)

Phys. Plasmas **21**, 063106 (2014); 10.1063/1.4882684

[Terahertz radiation by beating Langmuir waves](#)

Phys. Plasmas **19**, 114503 (2012); 10.1063/1.4769105

[Tunable and collimated terahertz radiation generation by femtosecond laser pulses](#)

Appl. Phys. Lett. **99**, 251101 (2011); 10.1063/1.3666855

[Generation of coherent terahertz radiation in ultrafast laser-gas interactionsa\)](#)

Phys. Plasmas **16**, 056706 (2009); 10.1063/1.3134422

[Hard-wall potential function for transport properties of alkali metal vapors](#)

J. Chem. Phys. **126**, 014302 (2007); 10.1063/1.2403879

An advertisement for Edmund Optics featuring a man in a blue shirt standing next to a piece of laboratory equipment. The background is dark with a blue diagonal banner in the top right corner. The text is in yellow and white.

NEED FREE PRODUCTS FOR YOUR LAB?

HURRY!
FINAL WEEKS TO APPLY

• 45 Global Educational Awards Available

www.edmundoptics.com/award **APPLY NOW!** TAKES ONLY 6 MINUTES. **eo Edmund optics | worldwide**

Terahertz radiation in alkali vapor plasmas

Xuan Sun and X.-C. Zhang^{a)}

Institute of Optics, University of Rochester, Rochester, New York 14627, USA

(Received 20 April 2014; accepted 28 April 2014; published online 13 May 2014)

By taking advantage of low ionization potentials of alkali atoms, we demonstrate terahertz wave generation from cesium and rubidium vapor plasmas with an amplitude nearly one order of magnitude larger than that from nitrogen gas at low pressure (0.02–0.5 Torr). The observed phenomena are explained by the numerical modeling based upon electron tunneling ionization.

© 2014 AIP Publishing LLC. [<http://dx.doi.org/10.1063/1.4876602>]

Far infrared radiation in the terahertz (THz) spectral region shows great potential for a large variety of applications^{1,2} ranging from molecular spectroscopy,³ material characterization,⁴ material engineering,⁵ imaging,⁶ to security screening.⁷ Lying at the heart of all these applications is THz wave generation and detection. In the past few decades, significant efforts have been devoted to develop a variety of THz wave sources,^{1–3,5,7,8} among which THz emission based upon gaseous plasmas⁸ exhibits a unique coherent broadband nature. In particular, its intriguing underlying physical mechanism and potential for standoff remote sensing excited significant interests in recent years to explore THz emission in a variety of gaseous media such as air,^{9–13} noble gases,^{14–16} and organic gases.¹⁷ However, the plasma-based emitters developed to date generally exhibit fairly low efficiencies and require a significant amount of pulse energy. For future practical application of THz air photonics, it is crucial to search for a gaseous medium with appropriate material characteristics for efficient THz wave generation. In this paper, we propose and demonstrate THz emission from cesium (Cs) and rubidium (Rb) vapor plasmas that are of great promise to be new material platforms for THz photonic application.

Cs and Rb vapors, with unique hyperfine energy level structures, are widely employed for nonlinear optics,¹⁸ atomic physics,¹⁹ frequency metrology,²⁰ and quantum information processing.²¹ However, little attention has been paid to their potential in THz application. Recent exploration of plasma filamentation^{15,22,23} indicates that the oscillation of plasma current associated with electron tunneling ionization is likely to be responsible for the THz emission in plasmas. This implies that the 1st ionization potential of a gaseous atom/molecule would play a critical role in THz wave generation since it determines directly the photo-ionization probability of the atom or molecule. With the nearly lowest ionization potentials among all fundamental elements (3.89 eV for Cs and 4.18 eV for Rb, in contrast to 15.58 eV for nitrogen gas),²⁴ Cs and Rb thus exhibit great potential for producing bright terahertz radiation.

So far, THz generation in gaseous media primarily focuses on the high-pressure regime aiming at producing a large THz field.^{8–17,25} However, it was shown recently^{8,17,25} that, in this regime, the linear dispersion, nonlinear phase modulation, and atom collisions of gaseous media can all

become significant enough to interfere seriously with THz emission. To reveal the essential performance of THz wave generation, here we explore the THz radiation in the low pressure regime, so that all these potential limiting perturbations are eliminated. The THz process therefore results primarily from the electron tunneling ionization of gaseous atom/molecule in response to the laser field.

We employ a dual-color laser scheme for terahertz generation.⁹ Figure 1 shows the schematic of our experimental setup. 50-fs laser pulses at 800 nm output from a regenerative Ti:Sapphire amplifier are launched into a 500- μm -thick β -barium borate (β -BBO) crystal to produce the second harmonic that co-propagates with the fundamental wave. Their relative dispersion induced by the system is compensated by an α -BBO crystal. The two color waves are adjusted by a dual-wavelength waveplate to be linearly copolarized and are then focused into the alkali vapor cell to produce plasma.

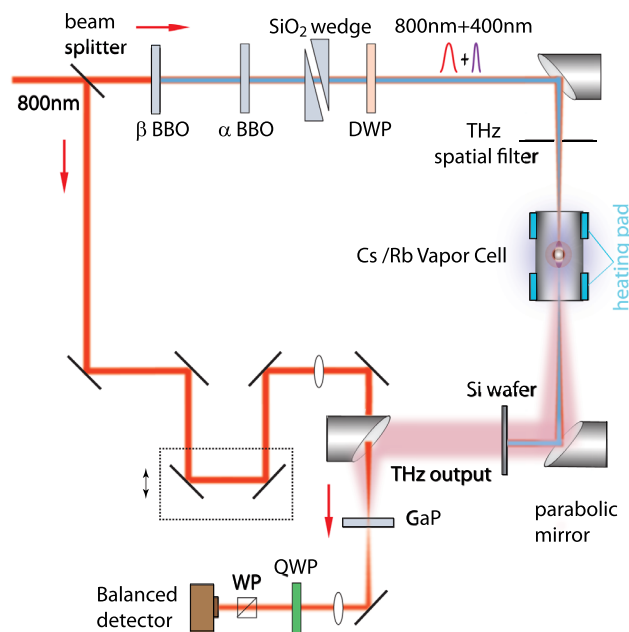


FIG. 1. Schematic of the experimental setup. DWP: dual-wavelength wave plate; QWP: quarter-wave plate; WP: Wollaston prism. The α -BBO is used to compensate the dispersion between the two-color waves. The SiO_2 wedge pair functions as an inline phase compensator to modulate the relative phase between the two-color waves. The two parabolic mirrors on the right have a focal length of 4 in. The THz spatial filter (an iris) is to block the residual THz wave emitted from β -BBO. The silicon wafer is used to block the residual two-color waves output from the cell. The vapor cell has two end windows made with 1.59-mm-thick fused silica.

^{a)}Electronic mail: Xi-Cheng.Zhang@rochester.edu.

The pressure of the alkali vapor is deduced from the vapor temperature.²⁶ The relative phase delay between the two color waves is precisely controlled by an in-line phase compensator²⁷ to optimize the THz emission. The produced THz wave is detected by electro-optic sampling via a 100- μm -thick GaP crystal using the 800-nm laser pulse as a probe. To calibrate the relative efficiency of THz generation in Cs and Rb vapors, we perform the same experiment in nitrogen gas under the same conditions, which functions as the reference.

Figure 2(a) shows an example of the recorded THz signal in Cs vapor when the relative two-color phase delay is changed. As expected, it shows the clear phase modulation feature, with an envelope determined by the pump pulse profile. Similar clear phase modulation is observed in Rb vapor. By setting the relative phase for the maximum THz output, we record the THz waveforms at different levels of vapor pressure. Figure 2(b) shows typical waveforms produced from the Cs and Rb vapors at a pressure of 0.45 Torr. Even

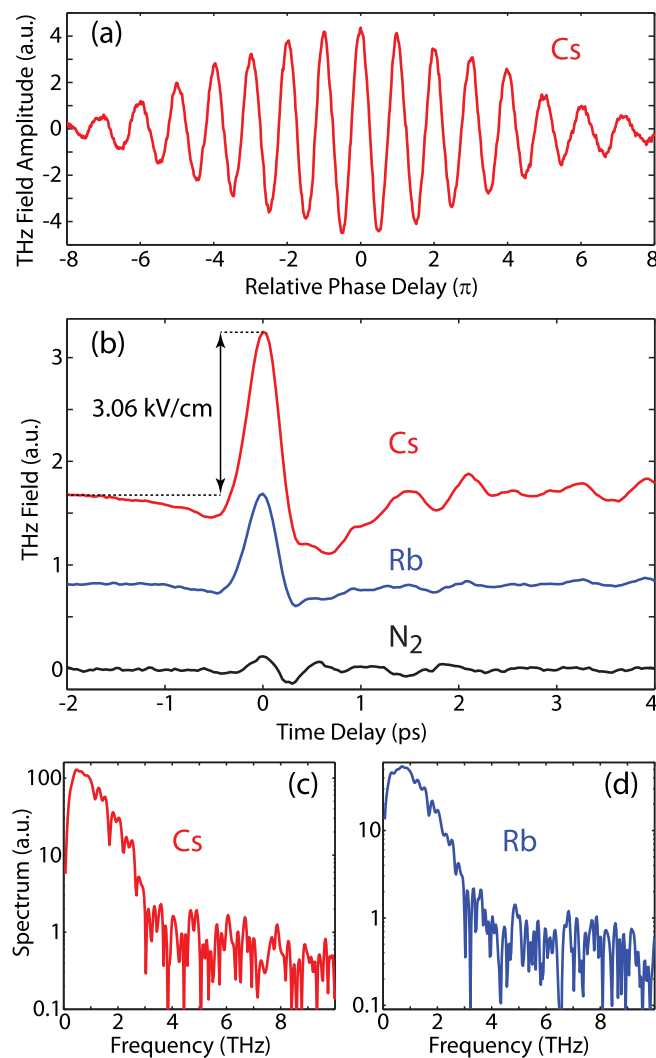


FIG. 2. (a) THz field amplitude produced in Cs vapor, as a function of relative two-color phase delay defined as $\frac{\omega\Delta L}{c}[n(2\omega) - n(\omega)]$, where ω is frequency of the fundamental wave, n is the refractive index, and ΔL is the length variation of the phase compensator. (b) THz time waveforms recorded at a pressure of 0.45 Torr with an input pulse energy of 0.6 mJ, produced in Cs vapor (red), Rb vapor (blue), and nitrogen gas (black), respectively. The indicated value refers to the THz field output from the cell. (c) and (d) The corresponding spectra for the THz pulses produced in Cs and Rb vapors, respectively.

at such a low pressure, both vapors are able to produce a pronounced THz waveform, with a signal to noise ratio of 120. The corresponding spectra (Figs. 2(c) and 2(d)) exhibit a bandwidth extending to above 2 THz. The spectral bandwidth is primarily limited by the absorption from the silica windows of the vapor cells.

Most importantly, Fig. 2(b) shows that the THz signals produced from the Cs and Rb vapors are significantly larger than that from nitrogen gas. This can be seen more clearly in Fig. 3, which plots the peak amplitudes of the THz fields versus vapor pressure. In general, THz signal increases linearly with pressure, in contrast to previous investigations,^{8–17,25} which confirms the advantage of exploring THz emission at low pressure. With all the interfering effects negligible, the THz signal depends linearly on the atom/molecule density. In particular, Rb vapor is able to produce THz signal about 3.6–6.4 times larger than nitrogen gas over the recorded pressure range. The signals produced from Cs vapor are even stronger, about 5.6–8.2 times larger than that from nitrogen.

To further explore the THz radiation behavior, we fixed the pressure at 0.45 Torr and recorded the peak amplitudes of the THz fields at various energy levels of the pump pulse, as shown in Fig. 4. In general, the THz field amplitude increases monotonically with input pulse energy till a certain level beyond which the THz field amplitude starts to saturate. However, Fig. 4 shows that the THz field amplitudes in Cs and Rb vapors are always larger than nitrogen for the recorded pulse energy from 0.06 to 0.6 mJ. For example, an input pulse with an energy of 0.4 mJ can produce a THz field amplitude of $\Delta I/I = 7.12 \times 10^{-4}$ and 4.16×10^{-4} in Cs and Rb vapors, respectively, while it can only reach a value of $\Delta I/I = 8.80 \times 10^{-5}$ in nitrogen (see the caption of Fig. 3 for the meaning of ΔI and I). Therefore, these alkali vapors are able to produce THz signal up to more than 8 times larger than nitrogen. As these gases have the same pressure and thus a nearly identical atom/molecule density, the THz

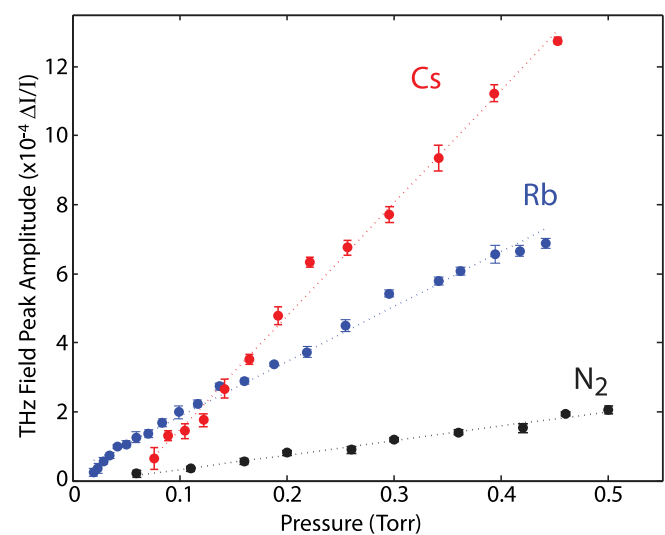


FIG. 3. Recorded peak amplitudes of THz pulses as a function of pressure, produced inside Cs vapor (red), Rb vapor (blue), and nitrogen gas (black). The input pulse energy is 0.6 mJ. The dashed lines are used for eye guidance. The vertical axis shows the differential output (ΔI) of the balanced detector for electro-optic sampling (Fig. 1) normalized by the averaged output (I) of its single detector. This ratio ($\Delta I/I$) gives the relative magnitude of detected THz field.

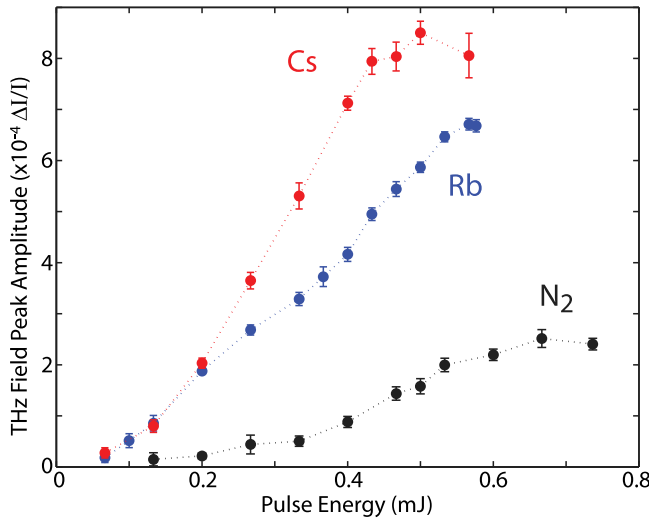


FIG. 4. Recorded peak amplitudes of THz pulses as a function of input pulse energy, produced inside Cs vapor (red), Rb vapor (blue), and nitrogen gas (black), at a pressure of 0.45 Torr. The dashed lines are used for eye guidance. The input pulse energy was recorded after the dual-wavelength waveplate (see Fig. 1) and thus corresponds to the total energy of the two color pulses.

emission efficiency per atom/molecule of alkali vapors is thus up to nearly one order of magnitude larger than that of nitrogen. These observations indicate that Cs and Rb vapors are good material candidates for potential THz photonic application.

To understand the physical mechanism underlying the strong THz radiation, we carried out theoretical investigation to estimate the THz generation efficiency. The observed strong THz radiation in the Cs and Rb vapors can be well understood with the plasma current oscillation associated with the electron tunneling ionization.²² In general, the produced THz field amplitude (E_{THz}) is determined by the time derivative of plasma current (J) which depends linearly on both the drift velocity (v_d) and the photo-ionization rate (w) of electrons: $E_{\text{THz}} \propto \frac{dJ}{dt} = ev_d(t)w(t)(\rho_0 - \rho_e(t)) \approx ev_d(t)w(t)\rho_0$, where ρ_0 and ρ_e are the densities of gas atom/molecule and ionized electron, respectively. The last approximation is valid in the undepleted region of gas ionization. As the drift velocity is primarily determined by the electric field of the dual-color waves, which is independent of gas species, the magnitude of the THz field thus relies essentially on the photo-ionization rate of the atom/molecule.

It is well known that the Perelomov-Popov-Terent'ev model provides an excellent description of the photo-ionization process, with an ionization rate given by^{23,28,29}

$$w = \omega_H \sqrt{\frac{6}{\pi}} |C_{n^*,l^*}|^2 f(l, m) A_m(\omega, \gamma) \frac{U_i}{2U_H} \times \left[\frac{2E_0}{E\sqrt{1+\gamma^2}} \right]^{2n-|m|-3/2} \exp\left[-\frac{2E_0}{3E} g(\gamma)\right], \quad (1)$$

where E is the electric field of the input laser with a frequency ω , $E_0 = E_H \left(\frac{U_i}{U_H}\right)^{3/2}$ represents the atomic field of the atom with an ionization potential of U_i . ω_H , E_H , and U_H are the atomic frequency, the atomic field, and the ionization potential of hydrogen atom. $\gamma = \left(\frac{U_i}{2U_p}\right)^{1/2}$ is the Keldysh

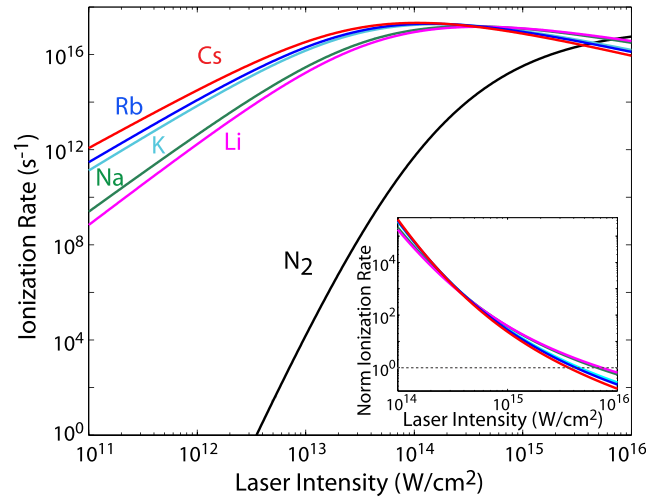


FIG. 5. Theoretical photo-ionization rates of Cs, Rb, K, Na, Li, and nitrogen atom as a function of laser intensity, calculated from Eq. (1). The photo-ionization is assumed to be dominated by the fundamental wave at 800 nm. The inset shows the photo-ionization rates of various alkali atoms normalized by that of nitrogen.

parameter with a ponderomotive energy of $U_p = \frac{e^2 F^2}{4m_e \omega^2}$. Equation (1) is adopted from Eq. (77) of Ref. 23 (and Eq. (8) of Ref. 29), which also provides the details of C_{n^*,l^*} , $f(l, m)$, $A_m(\omega, \gamma)$, and $g(\gamma)$.

Figure 5 compares the ionization rates of Cs and Rb, as well as other alkali atoms (potassium (K), sodium (Na), and lithium (Li)), with that of nitrogen, calculated from Eq. (1). It can be seen that the ionization rates of Cs and Rb increase monotonically with laser intensity until a certain intensity level beyond which it starts to saturate. This agrees qualitatively with the power-dependence shown in Fig. 4. In particular, the photo-ionization rates in Cs and Rb vapors are significantly higher than that of nitrogen for laser intensity up to $3 \times 10^{15} \text{ W/cm}^2$, thus verifying the stronger THz radiation in Cs and Rb vapors. K, Na, and Li show very similar behaviors. Figure 5 infers that, compared with nitrogen, alkali vapors would require considerably less optical intensity to achieve the same photo-ionization probability. Therefore, alkali vapors would be more energy efficient for THz wave generation. This

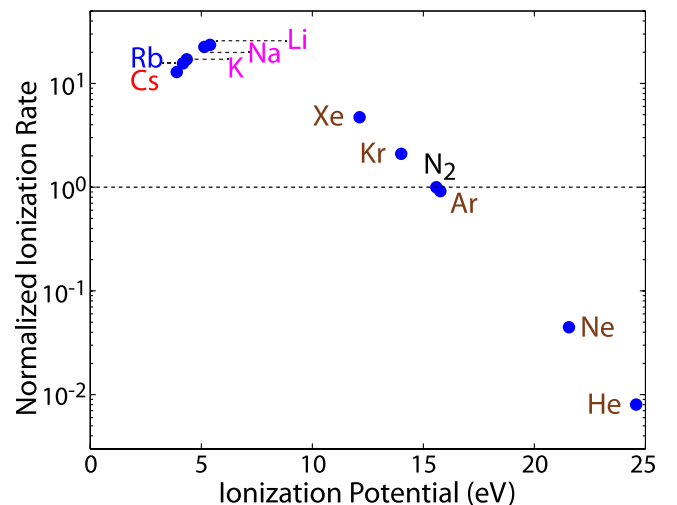


FIG. 6. Theoretical photo-ionization rates of different gases normalized by that of nitrogen, calculated from Eq. (1), with an input laser intensity of $1.22 \times 10^{15} \text{ W/cm}^2$.

would be particularly advantageous in future practical applications where energy efficiency becomes crucial.

The waist diameter of the focused beam in our experiment is estimated to be $\sim 30 \mu\text{m}$. As a result, a pump energy of 0.5 mJ corresponds to a laser peak intensity of $\sim 1.22 \times 10^{15} \text{ W/cm}^2$, after correcting the transmission of the front silica window of the vapor cell. Figure 6 compares the calculated ionization rate of various gaseous media at this intensity, normalized by that of nitrogen. It shows clearly that alkali vapors have considerably higher photo-ionization probabilities compared with all noble gases and nitrogen. More specifically, the ionization rates in Cs and Rb are about 13-16 times larger than nitrogen. These values agree closely with our experimental observation. The theoretical value in Cs slightly lower than that in Rb and other alkali atoms is because of laser-induced saturation (see Fig. 5). The lower value in Rb vapor observed in experiment is likely due to the absorption of the 800-nm input pulses by the Rb D transition lines whose wavelengths are very close to 800 nm.²⁶

In summary, we have demonstrated a scheme for terahertz wave generation, by taking advantage of extremely low ionization potentials in Cs and Rb vapors. We are able to produce a THz signal in Cs and Rb vapors up to nearly one order of magnitude larger than that in nitrogen under the same pressure. The observed phenomena are well explained by the theoretical modeling based on electron photo-ionization. The demonstrated THz radiation implies that alkali vapor plasmas may not only function as efficient THz emitters and detectors,¹⁷ but may also offer a unique access and insight into nonlinear THz dynamics in vapor plasmas. Although low-pressure vapors were used here to demonstrate THz emission, with appropriate packaging,³⁰ alkali vapors can be produced at relatively high pressures (say, tens of Torr) for intense THz emission. Therefore, future development of high-pressure vapor cells would render alkali vapors a promising material platform for THz photonic application.

This work was partially supported by the Army Research Office-Multidisciplinary University Research Initiative, the Defense Threat Reduction Agency, and National Science Foundation.

¹B. Ferguson and X.-C. Zhang, *Nature Mater.* **1**, 26 (2002).

²M. Tonouchi, *Nat. Photonics* **1**, 97 (2007).

- ³P. U. Jepsen, D. G. Cooke, and M. Koch, *Laser Photonics Rev.* **5**, 124 (2011).
- ⁴M. Naftaly and R. E. Miles, *Proc. IEEE* **95**, 1658 (2007).
- ⁵T. Kampfrath, K. Tanaka, and K. Nelson, *Nat. Photonics* **7**, 680 (2013).
- ⁶W. L. Chan, J. Diebel, and D. M. Mittelman, *Rep. Prog. Phys.* **70**, 1325 (2007).
- ⁷H. Liu, H. Zhong, N. Karpowicz, Y. Chen, and X.-C. Zhang, *Proc. IEEE* **95**, 1514 (2007).
- ⁸M. D. Thomson, M. Krebs, T. Löffler, and H. G. Roskos, *Laser Photonics Rev.* **1**, 349 (2007).
- ⁹D. J. Cook and R. M. Hochstrasser, *Opt. Lett.* **25**, 1210 (2000).
- ¹⁰M. Kress, T. Löffler, S. Eden, M. Thomson, and H. G. Roskos, *Opt. Lett.* **29**, 1120 (2004).
- ¹¹Y. Chen, T. Wang, C. Marceau, F. Theberge, M. Chateaufneuf, J. Dubois, O. Kosareva, and S. L. Chin, *Appl. Phys. Lett.* **95**, 101101 (2009).
- ¹²Y. Minami, T. Kurihara, K. Yamaguchi, M. Nakajima, and T. Suemoto, *Appl. Phys. Lett.* **102**, 041105 (2013).
- ¹³M. Clerici, M. Peccianti, B. e. Schmidt, L. Caspani, M. Shalaby, M. Giguère, A. Lotti, A. Couairon, F. Légaré, T. Ozaki, D. Faccio, and R. Morandotti, *Phys. Rev. Lett.* **110**, 253901 (2013).
- ¹⁴Y. Chen, M. Yamaguchi, M. Wang, and X.-C. Zhang, *Appl. Phys. Lett.* **91**, 251116 (2007).
- ¹⁵K. Y. Kim, A. J. Taylor, J. H. Glowina, and G. Rodriguez, *Nat. Photonics* **2**, 605 (2008).
- ¹⁶C. D. Amico, A. Houard, S. Akturk, Y. Liu, J. Le Bloas, M. Franco, B. Prade, A. Couairon, V. T. Tikhonchuk, and A. Mysyrowicz, *New J. Phys.* **10**, 013015 (2008).
- ¹⁷X. Lu, N. Karpowicz, and X.-C. Zhang, *J. Opt. Soc. Am. B* **26**, A66 (2009).
- ¹⁸M. Fleischhauer, A. Imamoglu, and J. P. Marangos, *Rev. Mod. Phys.* **77**, 633 (2005).
- ¹⁹A. D. Cronin, J. Schmiedmayer, and D. E. Pritchard, *Rev. Mod. Phys.* **81**, 1051 (2009).
- ²⁰S. A. Diddams, J. C. Bergquist, S. R. Jefferts, and C. W. Oates, *Science* **306**, 1318 (2004).
- ²¹N. Sangouard, C. Simon, H. de Riedmatten, and N. Gisin, *Rev. Mod. Phys.* **83**, 33 (2011).
- ²²K. Y. Kim, J. H. Glowina, A. J. Taylor, and G. Rodriguez, *Opt. Express* **15**, 4577 (2007).
- ²³A. Couairon and A. Mysyrowicz, *Phys. Rep.* **441**, 47 (2007).
- ²⁴*CRC Handbook of Chemistry and Physics*, edited by D. R. Lide, 84th ed. (CRC Press, 2003).
- ²⁵G. Rodriguez and G. L. Dakovski, *Opt. Express* **18**, 15130 (2010).
- ²⁶D. A. Steck, "Cesium D line data," Technical Report No. LA-UR-03-7943, Los Alamos National Laboratory, 2003; "Rubidium-87 D Line Data," Technical Report No. LA-UR-03-8638, Los Alamos National Laboratory 2003.
- ²⁷J. Dai, N. Karpowicz, and X.-C. Zhang, *Phys. Rev. Lett.* **103**, 023001 (2009).
- ²⁸A. M. Perelomov, V. S. Popov, and M. V. Terent'ev, *Sov. Phys. JETP* **23**, 924 (1966).
- ²⁹F. A. Ilkov, J. E. Decker, and S. L. Chin, *J. Phys. B: At., Mol. Opt. Phys.* **25**, 4005 (1992).
- ³⁰V. O. Lorenz, X. Dai, H. Green, T. R. Asnicar, and S. T. Cundiff, *Rev. Sci. Instrum.* **79**, 123104 (2008).